LARGE-BREAK LOCA ASSESSMENT FOR THE HIGHLY ADVANCED CORE DESIGN

F.J. DORIA, V.I. NATH, K.F. HAU, R.F. DAM AND J. VECCHIARELLI

Atomic Energy of Canada Limited (AECL)
2251 Speakman Drive, Mississauga
Ontario, Canada, L5K 1B2

ABSTRACT

Over the course of the years, a conceptual highly advanced core (HAC) reactor has been designed for Japan's Electric Power Development Company Limited (EPDC). The HAC reactor, which is capable of generating 1326 MW of electrical power, consists of 640 CANDU®-type fuel channels with each fuel channel containing twelve 61-element fuel bundles. As part of the conceptual design study, the performance of the HAC reactor during a large loss-of-coolant accident (LOCA) was assessed with the use of several computer codes. The SOPHT, CATHENA, ELOCA and ELESTRES computer codes were used to predict the thermalhydraulic behaviour of the circuit, thermalhydraulic behaviour of a single high-power channel, thermal-mechanical behaviour of the outer fuel elements contained in the high-powered channel, and the steady-state fuel-element conditions respectively. The LOCAs that were analyzed include 100% reactor outlet header (ROH) break, and a survey of reactor inlet header (RIH) breaks ranging from 5% to 25%. The conceptual feasibility of the HAC design was evaluated against two criteria; namely, maximum sheath temperature less than 1200°C and AECL's 5% sheath straining criterion to assess failure by excessive straining. For the cases analyzed, the analysis predicted a maximum sheath temperature of 820°C and a maximum sheath strain of 1.5% (the maximum pressure-tube temperature was 515°C).

Although the maximum element-burnup of the HAC design is extended beyond the CANDU 6 burnup, the maximum linear power of HAC (40 kW/m) is significantly lower than the maximum linear power of a CANDU 6 reactor (60 kW/m). The reduced element-power level in conjunction with internal design modification for the HAC design has resulted in significantly lower internal gas pressures under steady-state conditions, as compared with the CANDU 6 design. During a LOCA, the low linear powers and zero-void reactivity associated with the HAC design has increased the safety margin. In addition, the cases analyzed indicate that the reactor conditions (reactor power transient and flow conditions) during the transient do not lead to any significant increase in fuel volumetric-average temperature relative to the steady-state.

1. HIGHLY ADVANCED CORE DESIGN

The highly advanced core (HAC) design[1] involves a number of design modifications that have increased the safety margin. The following provides a brief summary of the HAC design:

- The bundle consists of 61 elements, contained in a 5-ring configuration.
- The outer 3 fuel rings contain low enriched uranium-235, and the inner 2 rings contain depleted uranium-235 and burnable poison. The amount of burnable poison in the inner 7 fuel elements is chosen to give an essentially zero-void reactivity.
- The pellet design has been optimized with the intent of minimizing the internal gas pressure.
- Graphite disks have been inserted between fuel pellets to provide low-resistance heat

---

CANDU® : Canada Deuterium Uranium is a registered trademark of Atomic Energy of Canada Limited.

conductive pathways away from the fuel and reduce fuel temperatures during normal operating conditions.

- The average bundle discharge burnup, maximum bundle discharge burnup and maximum element discharge burnup are 984 MW•h/kg U, 1200 MW•h/kg U and 1320 MW•h/kg U respectively.
- The maximum bundle power, maximum channel power and maximum element linear power are 975 kW, 7370 kW and 40 kW/m respectively.

2. DISCIPLINE INTERACTION

The SOPHT[2], CATHENA[3,4], ELOCA[5,6] and ELESTRES[7] computer codes are used to predict the behaviour of the HAC design during a loss-of-coolant accident (LOCA). The SOPHT circuit model predicts the primary heat transport system behaviour following a postulated reactor header break, including transient header conditions. Some of the important variables determined are core refilling time, break discharge rate and enthalpy, timing of safety system actions, coolant flow, pressure, temperature and inventory. The CATHENA single-channel simulation uses the SOPHT transient header conditions (pressure, enthalpy and void) and power transient as boundary conditions[8] to assess the single-channel thermalhydraulics in extensive detail. In order to assess the fuel behaviour during the transient, ELESTRES calculations are performed to estimate steady-state fuel-element conditions at the onset of the accident. Then, after the onset of the accident, the fuel and fuel-sheath behaviour of the outer fuel elements residing in the core pass downstream of the break (i.e., critical core pass) are evaluated by the ELOCA code. The ELOCA code requires information regarding the fuel-element state during normal operating conditions, which is obtained from ELESTRES. It also requires the power transient (obtained from SOPHT), coolant temperature, coolant pressure and sheath–to–coolant heat transfer coefficients (obtained from CATHENA) as transient boundary conditions. The interaction between the various disciplines is provided in Figure 1. The objective of this paper is to describe the methodology and provide the key results related to the single-channel assessment (i.e., CATHENA, ELESTRES and ELOCA simulations).

3. CATHENA SINGLE-CHANNEL ANALYSIS METHODOLOGY

The single-channel analysis is performed using the CATHENA thermalhydraulic computer code. CATHENA is a one–dimensional, two–fluid non–equilibrium thermalhydraulic computer code designed for the analysis of two–phase flow and heat transfer in piping networks. The model consists of individual mass, momentum, and energy equations for the gas and liquid phases, together with flow–regime dependent constitutive relations that describe mass, momentum, and energy transfers across the interface and between each phase and piping walls. The heat transfer process models available include wall and fuel heat conduction, heat generation through the zirconium metal–water reaction, thermal radiation heat transfer, wall–to–fluid heat transfer, and the heat transfer phenomena in a horizontal fuel channel during stratified flow conditions.

The CATHENA nodalization, which consists of the reactor inlet header, inlet feeders, inlet end–fittings, fuel channel, outlet end–fitting, outlet feeders, and reactor outlet header, is shown in

Figure 2. The inlet and outlet feeder is divided into 7 sections, the inlet and outlet end–fittings are divided into 4 sections, and the fuel channel is divided into 12 sections (i.e., 12 bundles residing within the channel). A detailed nodalization of the fuel elements, pressure tube, and calandria tube is provided in Figure 3. The nodalization considers that the fuel bundle, pressure tube and calandria tube are symmetrical across the vertical plane. Each fuel element is divided into 4 radial regions: fuel, gap, Zircaloy sheath and oxide layer. The fuel element model consists of a detailed radial nodalization with 6 radial nodes in the fuel pellet region, 2 radial nodes in the gap region, 2 radial nodes in the sheath region, and 2 radial nodes in the oxide region. The thermal radiation among the fuel elements, between the fuel elements and the pressure tube, and between the pressure tube and calandria tube is modelled in the CATHENA single-channel analysis; therefore, a view factor matrix associated with the HAC 61–element bundle design was generated. The heat transfer associated with a particular surface under flow stratification in the channel has been modelled by incorporating the appropriate channel void fractions used to calculate the heat transfer from surfaces submerged in liquid and the heat transfer from surfaces exposed to steam conditions.

A detailed physics calculation was performed to determine the axial power profile for the high–powered channel. The axial power profile for the channel was determined at the state of highest channel power observed in the physics 1000 full-power days (FPD) simulation (i.e., the maximum channel power of 7.4 MW occurs at 840 FPDs). Since each ring of fuel elements was simulated in CATHENA, the axial power profile of each ring was applied in the simulation. The maximum channel power was arbitrarily increased from 7.4 MW to 7.7 MW to account for uncertainties.

4. FUEL ANALYSIS METHODOLOGY

In order to assess the fuel behaviour during the transient, the dynamic response of the fuel element must be considered. That is, phenomena such as sheath deformation, fuel-to-sheath heat transfer coefficient and internal gas pressure should be recognized in the analysis. Since a detailed fuel model is not available in CATHENA, the ELESTRES and ELOCA code were used to simulate the fuel behaviour for the 100% reactor outlet header (ROH) and 5 reactor inlet header (RIH) break cases. For some breaks, the coolant flow in the core pass downstream of the break is significantly reduced for a short period of time. The reduced flow rate results in a decreased fuel-to-coolant convective heat transfer and subsequent increase in sheath temperatures. A rise in sheath temperatures reduces the sheath strength, and the pressure gradient across the sheath increases the stress applied to the fuel sheath. The increased fuel-sheath stress and decreased fuel-sheath strength may result in sheath straining in the critical core pass.

4.1 Fuel-Element Steady-State Conditions

The ELESTRES code models the behaviour of CANDU fuel elements under normal operating conditions. The code requires the geometrical data of the fuel element, coolant boundary conditions and a power–burnup history as input. Some of the important performance parameters include fission–gas release, internal and interfacial pressures, temperature and pellet ridge strains. A single element is modelled by accounting for the radial and axial variations in stresses and displacements. The constituent equations are physically based and include such phenomena as

pellet–to–sheath heat transfer, temperature and porosity dependence of pellet thermal conductivity, burnup–dependent neutron–flux depression, burnup– and microstructure–dependent fission–product gas release, and stress–, dose– and temperature–dependent constitutive equations for the sheath. The interactions and feedbacks among these parameters are considered in a dynamic manner throughout the irradiation history.

Fuel-element initial conditions are determined by using a modified version of the ELESTRES computer code, which accounts for the presence of the HAC inter–pellet graphite disc by allowing heat flow to be conducted in the radial, axial and circumferential directions. In order to determine the pre–transient fuel conditions for the 100% ROH and the five RIH breaks, a total of 12 ELESTRES cases that simulate the outer elements of the 12 bundles residing within the high-powered channel were completed.

The ELESTRES cases simulated the fuel behaviour during normal operating conditions using the high–powered envelope and the outer-element burnups obtained for the highest powered channel. A high–power envelope is a hypothetical power/burnup history that has a higher power history than the power history of any bundle in the core. For design assessments, a bundle will meet the continuous high–power requirements of the core for a particular refuelling scheme if it can be shown that a bundle will successfully operate along a power history outlined by the envelope. Based on results obtained from the 1000-FPD refuelling simulations, the maximum linear power of the HAC element is ≈40 kW/m at a burnup of ≈240 MW•h/kg U. For assessing the fuel performance during normal operating conditions, the high–power envelope was arbitrarily pro–rated to a maximum linear power of 47 kW/m to account for simulation uncertainties and the axial flux peaking factor.

4.2 Transient Fuel and Sheath Behaviour

Analysis of the fuel and fuel–sheath behaviour during the LOCA was performed with the ELOCA.MK5 computer code. ELOCA.MK5 is used to simulate the transient thermo–mechanical response of a single fuel element following an accident. The model treats a single Zircaloy–sheathed UO_2 fuel element and assumes axisymmetrical properties. Physical effects considered in the ELOCA code are as follows: thermal, elastic and plastic sheath deformation; variation of internal gas pressure during the transient; variation of the fuel–to–sheath heat transfer coefficient and the fuel–to–sheath radial gap during the transient; fuel expansion, cracking and melting; beryllium–assisted crack penetration of the sheath; and sheath oxidation.

The ELOCA.MK5 analysis is used to evaluate the fuel performance against the fuel-sheath integrity requirements of maximum sheath temperature less than 1200°C, and AECL's 5% sheath straining criterion.

5. RESULTS OF THE 15% RIH ANALYSIS

Since the analysis indicates that the 15% RIH case results in the highest temperatures, detailed analysis results associated with this case are presented.

5.1 CATHENA Simulation

The boundary conditions (pressure, fluid enthalpy, vapour enthalpy and void) for the broken pass of the broken loop, which have been determined from the SOPHT circuit analysis, are applied in the CATHENA single-channel analysis. Since the broken reactor inlet header is RIH 4, the critical pass contains the channels between RIH 4 and ROH 1. The mass flow rate for channel R17, which is a channel in the critical pass, drops rapidly as a result of depressurizing RIH 4, and the mass flow rate in the broken pass reverses.

The maximum sheath temperatures calculated for each ring of elements of the HAC bundle indicate that the outer–element temperatures are the maximum in the channel (Figure 4). Furthermore, due to flow stratification in the channel, the maximum sheath temperature occurs in the element located at the top of the bundle. The CATHENA single-channel analysis indicates that the maximum sheath temperature during the transient is 769°C. A detailed ELOCA analysis of the fuel element is provided in Section 5.3.

The pressure-tube temperatures and radial stresses for each channel location are predicted by CATHENA. The pressure-tube temperatures during the transient closely follow the profile of the fluid temperatures, with a maximum pressure-tube temperature of 515°C.

5.2 Fuel-Element Initial Conditions (ELESTRES Simulations)

The power–burnup histories, which are based on the 1000–FPD physics simulation, are shown in Figure 5. The power level for each of the bundles is close to the power levels determined for the high-powered envelope, which is based on the element power levels of the entire core during the 1000–FPD physics simulation. Therefore, the power levels of each bundle are assumed to be represented by the power level associated with the high-powered envelope. Since the LOCA is assumed to occur at the time of highest channel power, the outer–element burnups of the bundles residing within channel R17 at 840–FPD are applied in the ELESTRES simulations. As the fuel burnup increases, the fission gas released to the gap is increased and the peak internal gas pressure increases (Table 1).

5.3 Fuel-Element Transient Behaviour (ELOCA Simulations)

The CATHENA single-channel simulations indicate that the top element of the outer ring in each bundle achieves the maximum fuel temperature; therefore, ELOCA simulations used the predicted CATHENA coolant pressure, coolant temperature and sheath–to–coolant heat transfer coefficient corresponding to these top elements in the outer ring of the 12 bundles residing in channel R17. The sheath temperatures predicted by ELOCA are provided in Figure 6. The

maximum sheath temperature predicted by ELOCA is 815°C; therefore, the 1200°C peak–sheath–temperature criterion has been satisfied. The fuel centreline temperature, fuel volumetric averaged temperature, fuel surface temperature, and the sheath temperature for the top elements in the outer ring of bundle 4 are provided in Figure 7. Early in the transient, the flow in the channel approaches stagnation and the sheath–to–coolant heat transfer is significantly reduced, resulting in an increase in the net heat flow into the sheath. The heat content within the fuel is rapidly redistributed (i.e., a decrease in the fuel centerline temperature with an increase in the fuel surface temperature) and therefore the sheath experiences a significant temperature rise. The increase in sheath temperature reduces the net influx, since the temperature gradient between the fuel surface and the sheath is reduced. The coolant flow moves away from the stagnation point and a reverse flow rate is established. The reverse flow results in an increase in heat removal from the sheath and the sheath temperature decreases. Later in the transient (≈20 s), the sheath experiences a second heat-up period resulting from near stagnation conditions. However, at this time the heat content within the fuel has been significantly reduced by the heat removal associated with the previous off-stagnation periods. At this point, the relatively slow heat-up indicates that the decay heat generated is slightly greater than the heat removed by convection and radiation.

An important parameter in determining the transient response of a sheath during a LOCA is the stored energy in the fuel element at the time of stagnation. To maximize the sheath temperature, the stored heat contained within the fuel element should be maximized at the time stagnation occurs. The maximum sheath temperature is limited to the fuel surface temperature, which is related to the volumetric-averaged fuel temperature. If there is significant cooling before stagnation occurs (i.e., energy removed from the element is greater than the energy generated), then the volumetric-averaged fuel temperature will decrease. Then, once near-stagnation conditions occur in the channel, the sheath temperature will increase and the fuel centreline temperature will decrease to this reduced volumetric-averaged fuel temperature (Figure 7).

5.3.1 Sheath Strains

The sheath strains predicted by ELOCA (Figure 8) are significantly below the 5% failure criterion; therefore, sheath failure caused by excessive straining is precluded. The sheath straining behaviour may be understood by identifying the underlying principles that govern the deformation of the sheath. In ELOCA, the total sheath strain is composed of three components: elastic straining (dependent on Young's modulus, hoop stress and axial stress), thermal expansion straining (dependent on the sheath temperature), and plastic/creep straining (based on experimental determined parameters for Zircaloy sheath material, hoop stress, axial stress, and the creeping behaviour of the sheath). The stresses and temperatures occurring during a LOCA transient may result in significant changes in the Zircaloy microstructure (grain size, dislocation density and phase changes from alpha–to–beta).[5] The creep behaviour of the Zircaloy sheath during a LOCA is dependent on these microstructural changes. The pre-transient analysis predicts that the sheath is in contact with the fuel pellet at the onset of the accident; however, a radial gap develops during the LOCA transient. In some elements, a rapid reduction in sheath strain at high sheath temperatures (i.e., sheath collapse onto the fuel pellet at ≈5 s) occurs and is related to the creep behaviour of the sheath (i.e., high sheath temperatures with the external coolant pressure being greater than the internal gas pressure).

6. REACTOR HEADER BREAK SUMMARY

The depressurization transient associated with the RIH of the critical pass illustrates the relative depressurization for the various breaks analyzed and effectively shows that the larger break sizes result in a faster depressurization of the header (Figure 9). The channel flow rates in the early portion of the transient indicate a rapid flow reversal for large breaks such as 25% RIH and 100% ROH, sustained forward flow for smaller breaks such as the 5% RIH, and near stagnation conditions for intermediate breaks such as 15%, 10% and 8% RIH (Figure 10). The profile of the maximum sheath temperatures, which correspond to bundle position 4 for all of the LOCA cases, are in direct response to the channel flow conditions (Figure 11).

An important parameter in the analysis is the "stored heat" within the fuel at the "time of stagnation". If the stagnation occurs early in the transient, then the stored heat is quite high, close to the steady–state value. If the stagnation occurs later in the transient, then the stored heat would have been reduced from the normal operating condition. However, if the stagnation period persists in the later portion of the transient, then the stored heat will increase as a function of duration of channel stagnation and heat generated by the fuel. The volumetric-averaged fuel temperature during the transient, which is a good indicator of stored heat, and the timing of the maximum sheath temperature are plotted for each of the LOCA cases in Figure 12. For each of the cases, the maximum sheath temperature is limited by the volumetric-averaged fuel temperature. It is interesting to compare the results for the 10% RIH and 8% RIH breaks. The smaller break size of 8% RIH, as compared with 10% RIH, results in a slower depressurization of the inlet header and therefore, the positive flow rate for the 8% break requires more time, as compared with the 10% break to reach the near-stagnation condition (≈10 s for 8% RIH, ≈5 s for 10% RIH). As shown in Figure 12, the additional cooling associated with the 8% RIH case, as compared with the 10% case, results in a lower volumetric-averaged temperature before stagnation. In both the 8% and 10% RIH cases, the volumetric-averaged fuel temperatures begin to increase following stagnation, which indicates that the heat removal is less than the heat generated by the fuel. Even though the stagnation period for the 8% RIH case (≈15 s of stagnation) is greater than the 10% RIH (a few seconds), the maximum volumetric-averaged fuel temperature following stagnation is lower for the 8% RIH, as compared to the 10% RIH. This is due to the initial reduction in volumetric-averaged temperature that resulted from convective cooling. For the range of break sizes considered, the stagnation period is insufficient to increase the sheath temperature beyond the 1200°C threshold. For all the reactor header breaks analyzed, the maximum sheath strain is less than ≈1.5% and the maximum pressure–tube temperature remains relatively low (less than ≈515°C).

7. CONCLUSIONS

The computer codes SOPHT, CATHENA, ELESTRES and ELOCA were used to predict the HAC performance during a LOCA. The LOCAs that were analyzed include 100% ROH, 25% RIH, 10% RIH, 5% RIH, 8% RIH and 15% RIH. The conceptual feasibility of the HAC design was evaluated against two criteria; namely, maximum sheath temperature less than 1200°C and AECL's 5% sheath straining criterion. The maximum sheath temperature for the cases analyzed is 816°C. The maximum sheath strain is less than ≈1.5% and the maximum pressure tube temperature remains relatively low (less than ≈515°C). The relatively low pressure tube

temperature in conjunction with the predicted pressure-tube stress (with the maximum stress occurring at the onset of the accident) is insufficient to result in pressure tube straining.

Although the maximum element-burnup of the HAC design is extended beyond the CANDU 6 burnup, the maximum linear power of HAC (40 kW/m) is significantly lower than the maximum linear power of a CANDU 6 reactor (60 kW/m). The reduced element-power level in conjunction with internal design modification for the HAC design has resulted in significantly lower internal gas pressures under steady-state conditions, as compared with the CANDU 6 design. During a LOCA, the low linear powers and zero-void reactivity associated with the HAC design has increased the safety margin. In order to violate the maximum sheath temperature criterion, then the volumetric-averaged fuel temperature would have to approach ≈1200°C. In all of the cases analyzed, the maximum volumetric-averaged fuel temperature at the onset of the accident is ≈1000°C. More importantly, the cases analyzed indicate that the reactor conditions (reactor power and flow conditions) during the transient do not result in any significant increase in fuel volumetric-averaged temperature relative to the steady–state fuel volumetric-averaged temperature.

8. ACKNOWLEDGEMENTS

The authors would like to thank EPDC for the financial contribution and technical discussions.

9. REFERENCES

[1] M. Tayal, J.W. Love, D. Dennier, M. Gacesa, S. Sato, J. MacQuarrie, B.A.W. Smith, S-D. Yu, M. Tanaka, B. Wong and C. Manu, *A 61-Element Fuel Design (HAC) for Very High Burnups*, Fourth Annual Conference on CANDU Fuel, Pembroke, Canada, 1995 October 1-4.

[2] C.Y.F. Chang and J. Skears, *SOPHT - A Computer Model for CANDU - PHWR Heat Transport Networks and Their Control*, Nuclear Technology, 35, 1977.

[3] B.N. Hanna, *CATHENA: A Thermalhydraulic Code for CANDU Analysis*, Nuclear Engineering and Design (publication accepted).

[4] D.J. Richards, B.N. Hanna, N. Hobson and K.H. Ardon, *ATHENA: a two-fluid code for CANDU LOCA analysis Proceedings of the* 3rd International Topical Meeting on Reactor Thermalhydrualics, Newport, Rhode Island, pp 7.E-1 to 7.E-14, 1985.

[5] H.E. Sills, *ELOCA Fuel Element Behaviour during High-Temperature Transients*, Atomic Energy of Canada Limited Report, AECL-6357, 1979 March.

[6] J. Walker, *The Calculation of Transient Fission Product Release from CANDU Fuel Elements Using the ELOCA.MK5 Code*, 12th Annual Conference of the Canadian Nuclear Society, Saskatoon, Saskatchewan, 1991 June 9-12.

[7] M. Tayal, *Modelling CANDU Fuel Under Normal Operating Conditions: ELESTRES Code Description*, Atomic Energy of Canada Limited Report, AECL-9331, 1987 February.

[8] J. Vecchiarelli, R.F. Dam, K.F. Hau and F.J. Doria, *Thermalhydraulic Response of a Conceptual CANDU Reactor with a Highly Advanced Core Subject to Various Loss-of-Coolant Accidents*, 20th Nuclear Simulation Symposium, Niagara on the Lake, Ontario, 1997 September.

Table 1: ELESTRES Predictions for Channel R17

PARAMETER	Bundle Position											
	1	2	3	4	5	6	7	8	9	10	11	12
Peak Element Power (kW/m)	46.5	46.6	47	47	47	47	47	47	47	47	47	47
Maximum Burnup (MW•h/kg U)	4	59	166	282	409	518	586	666	745	818	898	958
Element Power at Maximum Burnup (kW/m)	46.5	46.6	47	44.8	38.3	33.9	31.9	28.9	26.6	25.4	23.6	22.5
Peak Fuel Centreline Temperature (K)	1813	1813	1901	2039	2041	2041	2041	2041	2041	2041	2041	2041
Fuel Temperature at Maximum Burnup (K)	1810	1792	1900	2039	1936	1799	1750	1661	1590	1562	1509	1479
Gas Release at Maximum Burnup (mm^3)	0	84	1061	6398	12211	14539	15797	16975	18175	19025	20225	21068
Peak Internal Pressure (MPa)	0.37	0.38	0.65	2.09	3.85	4.27	4.44	4.75	5.2	5.49	5.97	6.42

Figure 1: Interaction between Disciplines for the LOCA Analysis

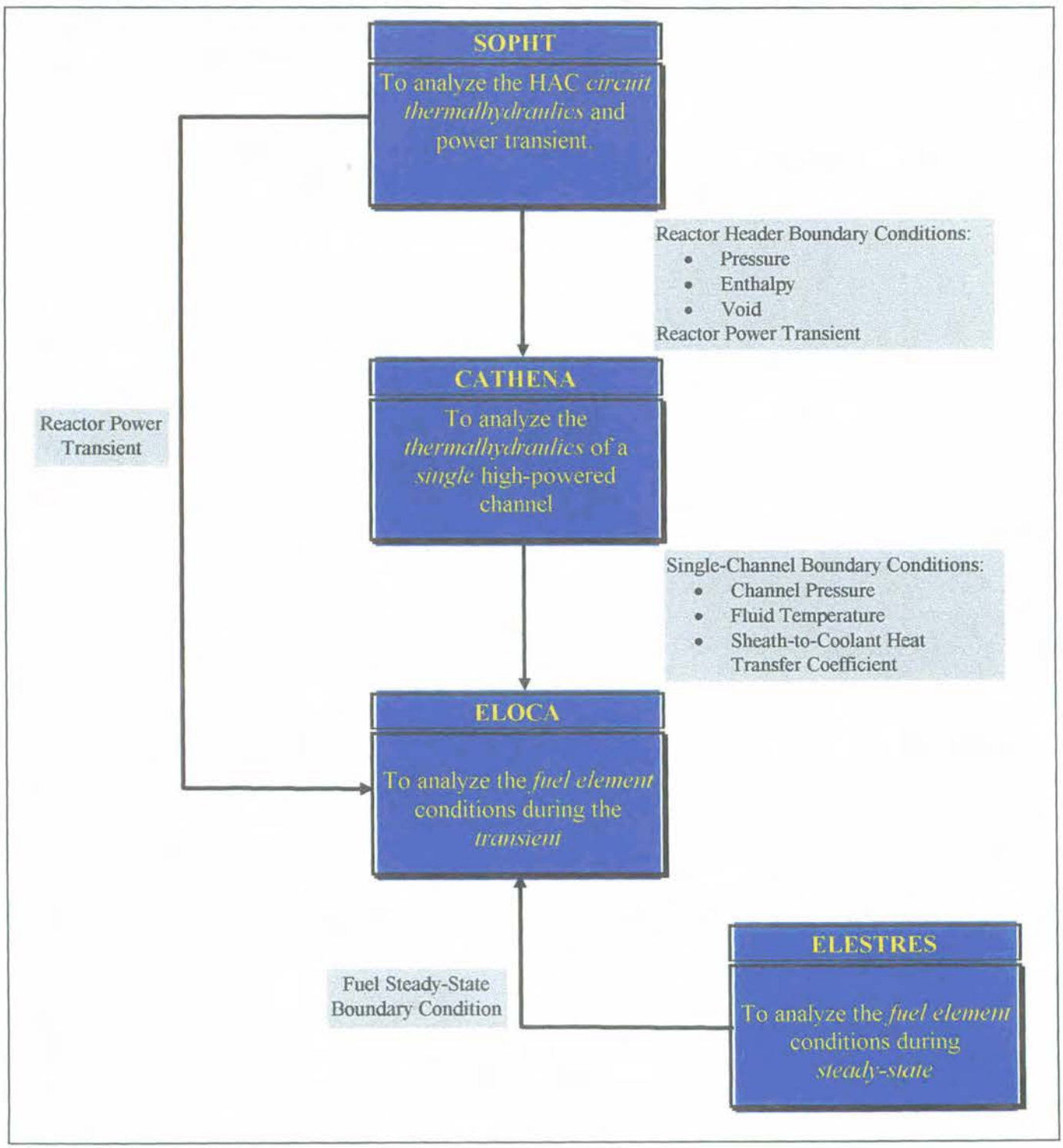

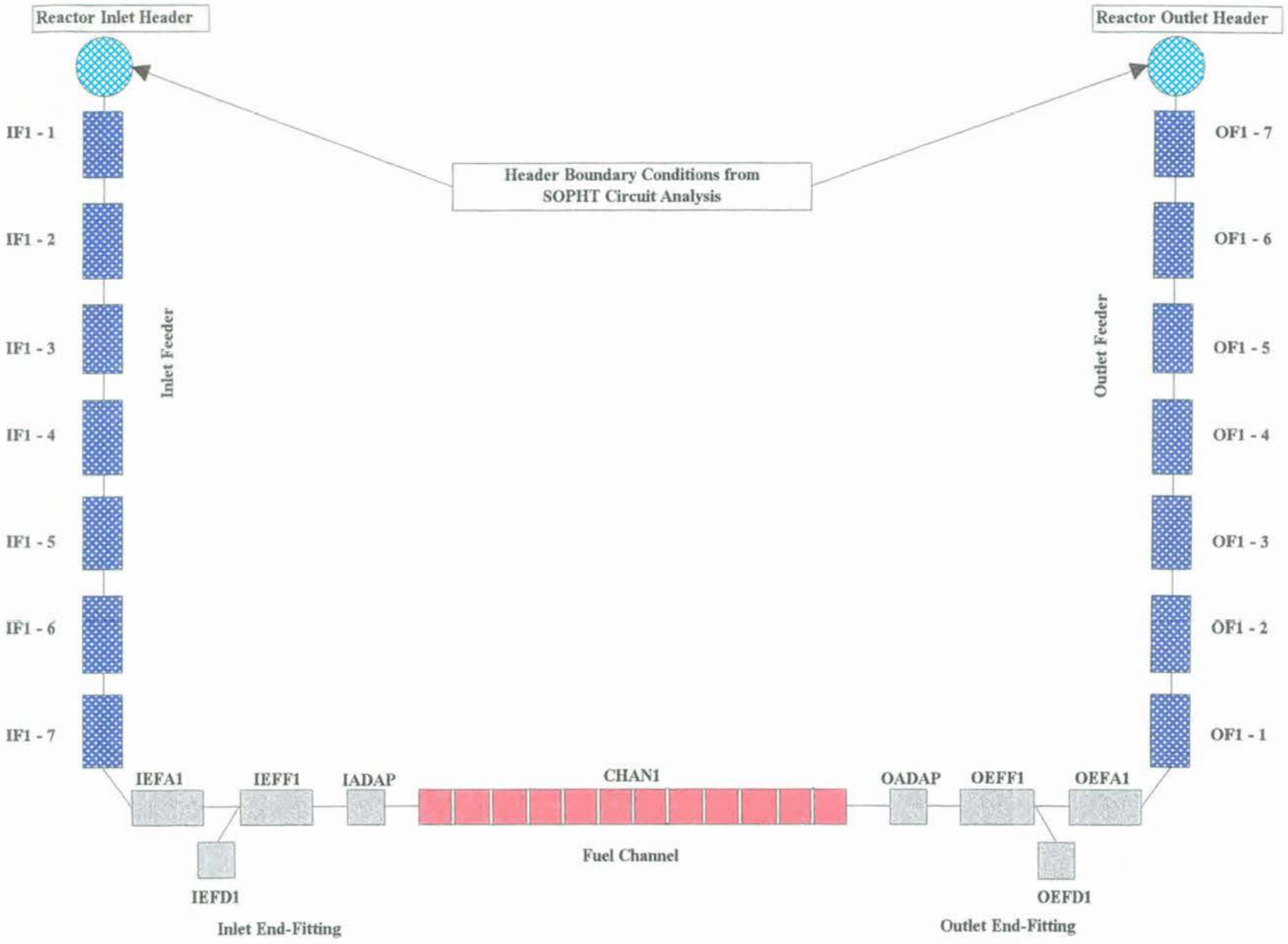

Figure 2: CATHENA Single-Channel Nodalization

Figure 3: Fuel Channel Representation in the CATHENA Single-Channel Model

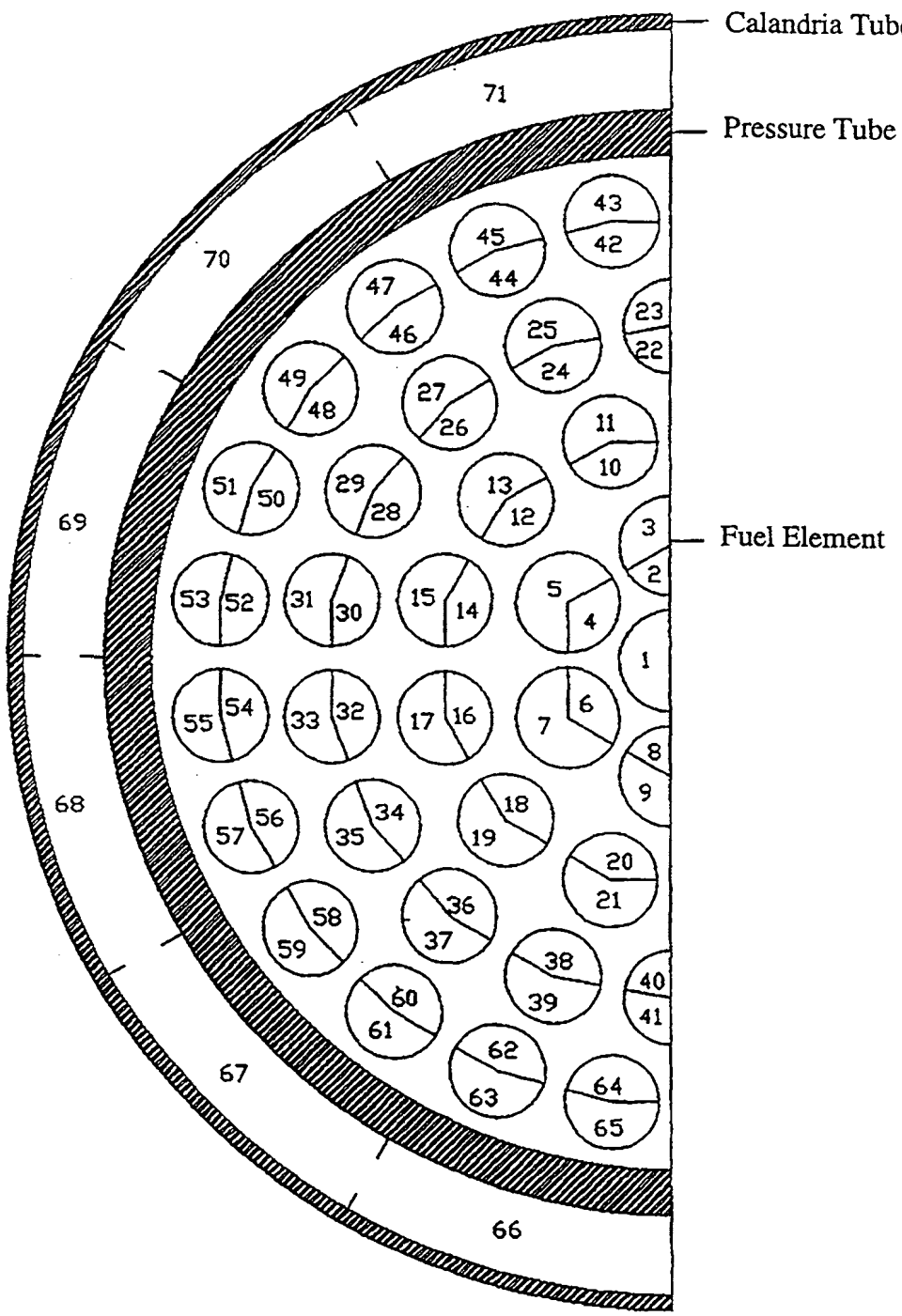

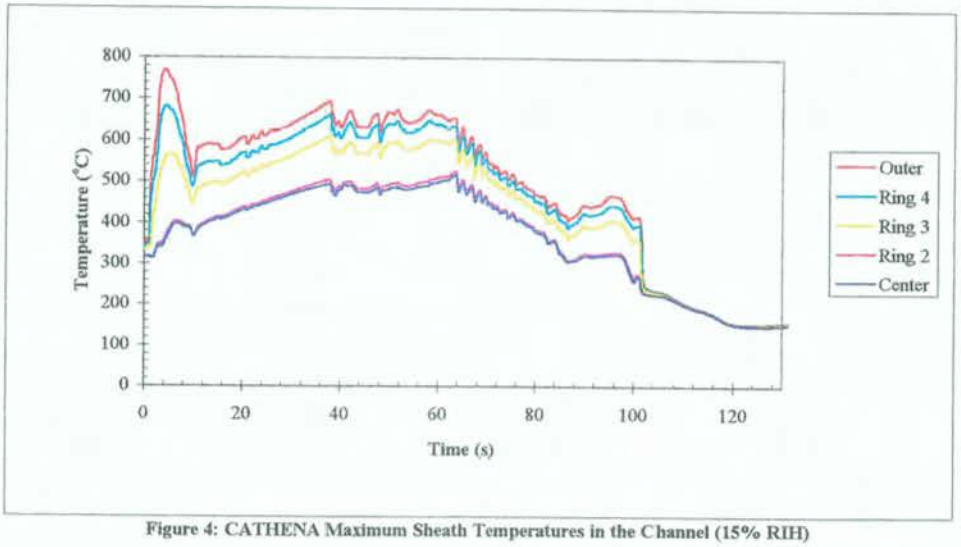

Figure 4: CATHENA Maximum Sheath Temperatures in the Channel (15% RIH)

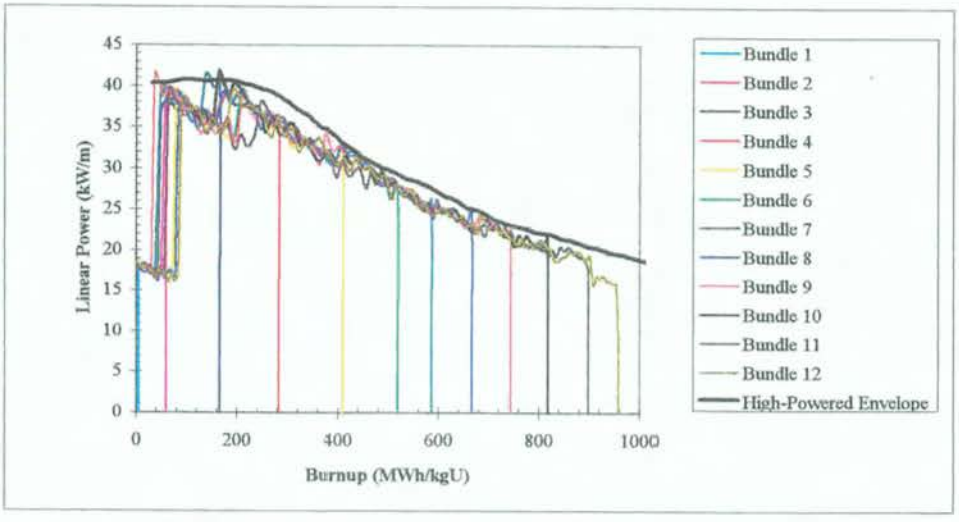

Figure 5: Power Histories for the Outer Elements in a High-Powered Channel up Until Onset of Accident at 840-FPD

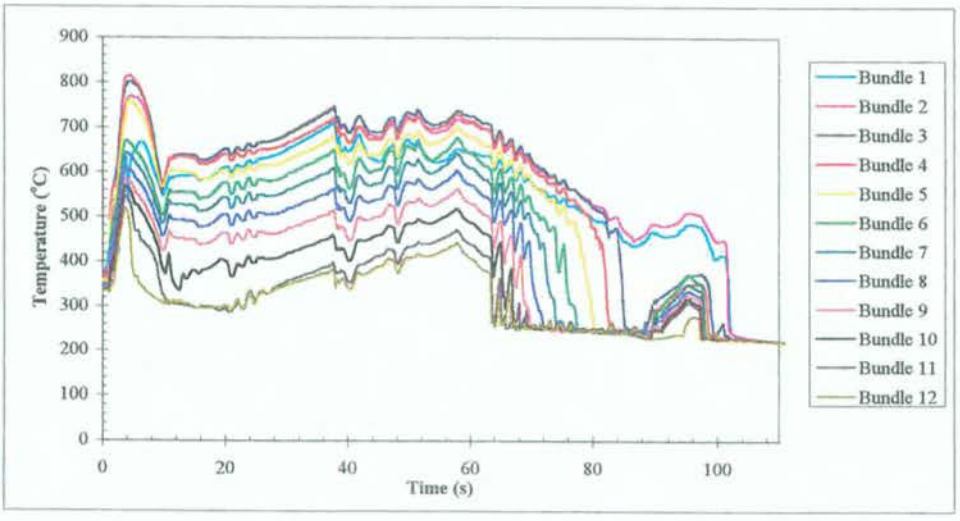

Figure 6: ELOCA Sheath Temperatures for the Top Element in the Outer Ring (15% RIH)

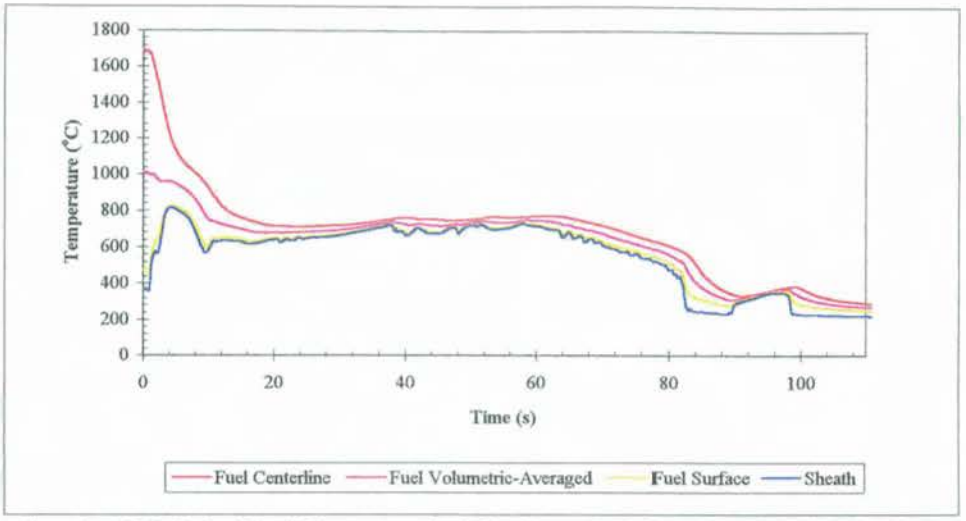

Figure 7: ELOCA Fuel and Sheath Temperatures for the Top Element in the Outer Ring of Bundle 4 (15% RIH)

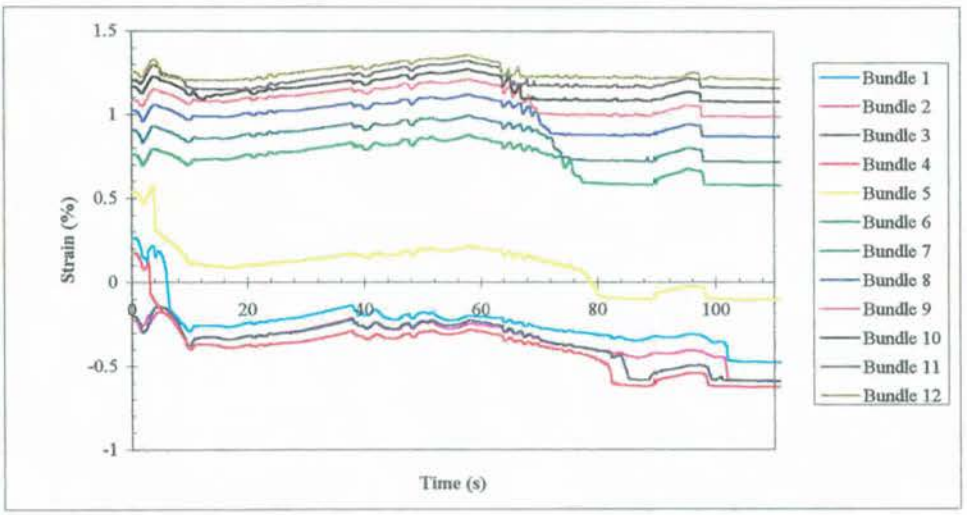

Figure 8: ELOCA Sheath Strain for the Top Element in the Outer Ring (15% RIH)

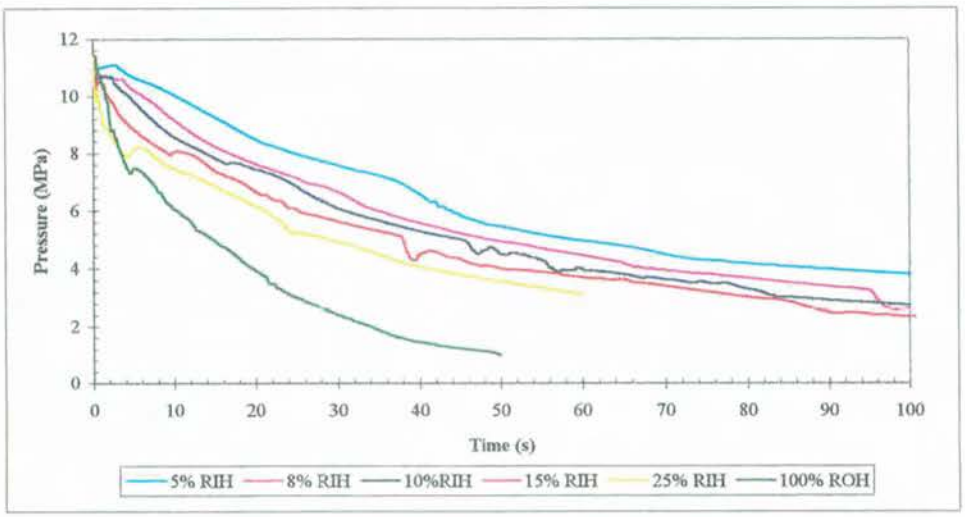

Figure 9: RIH Depressurization Transient for the Critical Pass

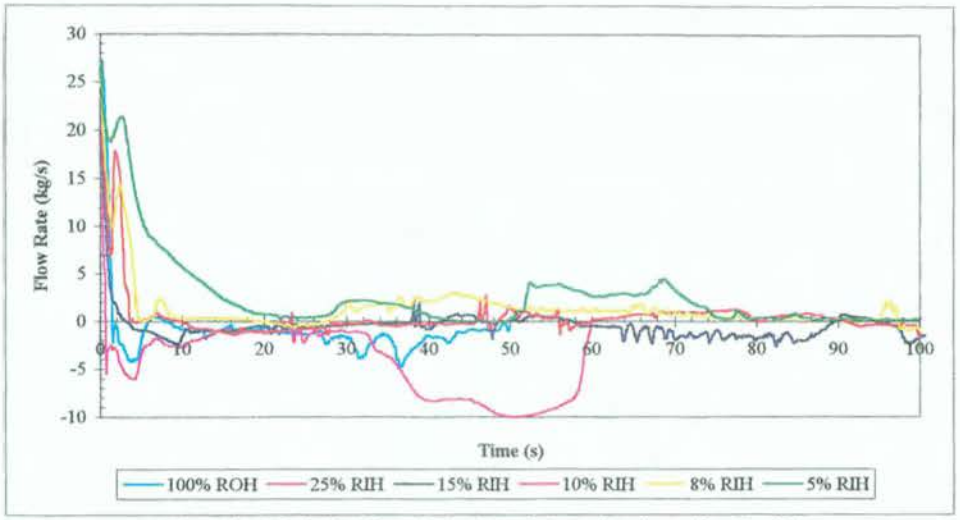

Figure 10: CATHENA Channel Flow Rates (between bundle position 3 and 4)

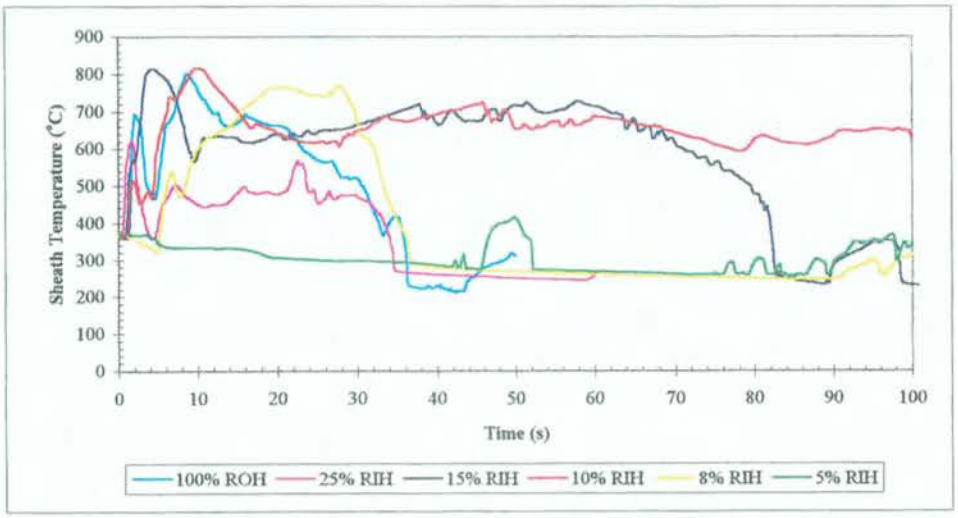

Figure 11: Summary of ELOCA Sheath Temperatures for the Top Element in the Outer Ring of Bundle 4

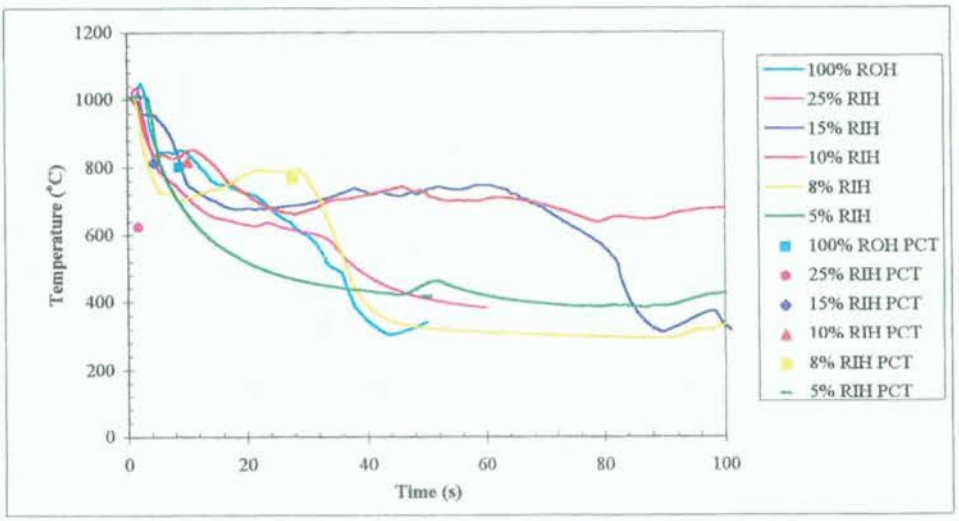

Figure 12: ELOCA Volumetric-Averaged Fuel Temperature and Maximum Sheath Temperature for the Top Element in the Outer Ring of Bundle 4